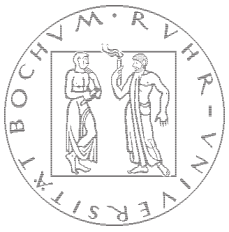

Preprint 01-2007

Variational h-adaption in finite deformation elasticity and plasticity

J. Mosler and M. Ortiz

This is a preprint of an article accepted by:

International Journal for Numerical Methods in Engineering (2007)

Ruhr University Bochum
California Institute of Technology

Variational h-adaption in finite deformation elasticity and plasticity

J. Mosler [*†]

Institute of Mechanics
Ruhr University Bochum
Universitätsstr. 150,D-44780 Bochum, Germany
E-Mail: mosler@tm.bi.ruhr-uni-bochum.de

M. Oritz[*]

Graduate Aeronautical Laboratories
California Institute of Technology
Pasadena, CA 91125, USA
E-Mail: ortiz@aero.caltech.edu

SUMMARY

We propose a variational h-adaption strategy in which the evolution of the mesh is driven directly by the governing minimum principle. This minimum principle is the principle of minimum potential energy in the case of elastostatics; and a minimum principle for the incremental static problem of elasto-viscoplasticity. In particular, the mesh is refined locally when the resulting energy or incremental pseudo-energy released exceeds a certain threshold value. In order to avoid global recomputes, we estimate the local energy released by mesh refinement by means of a lower bound obtained by relaxing a local patch of elements. This bound can be computed locally, which reduces the complexity of the refinement algorithm to $O(N)$. We also demonstrate how variational h-refinement can be combined with variational r-refinement to obtain a variational hr-refinement algorithm. Because of the strict variational nature of the h-refinement algorithm, the resulting meshes are anisotropic and outperform other refinement strategies based on aspect ratio or other purely geometrical measures of mesh quality. The versatility and rate of convergence of the resulting approach are illustrated by means of selected numerical examples.

1 INTRODUCTION

Mesh adaption for linear elliptic problems may be based on standard error estimates. In this context, adaptivity strives to minimize an error bound among all meshes of a fixed size; or by the recursive application of local refinement steps (cf, e. g., [1, 2] for reviews). Error estimation pre-supposes existence and uniqueness of the solution; relies strongly on the linearity of the problem; and in the corresponding Hilbert-space structure of the solution space. In addition, the standard error bounds require a certain regularity of the solution for their validity, and averaging over patches of elements is typically required in order to estimate the local errors (cf, e. g., [3]). Error estimates break down entirely when the solution lacks regularity; and when loss or near-loss of ellipticity occurs, e. g., as a consequence of localization instabilities.

If error estimation is not without difficulty in a linear framework, it is entirely inimical to strongly nonlinear problems involving finite kinematics. Indeed, these problems often lack uniqueness, owing to instabilities such as buckling, and even existence due to non-convexity arising from material instabilities, phase transitions and other root causes. Furthermore, the

[*]DoE through Caltech's ASC/ASAP Center
[†]Deutsche Forschungsgemeinschaft (DFG); contract/grant number: Mo 1389/1-1

topologies that are natural to these problems are often not normed, and the spaces where solutions are to be found may not have a linear structure at all.

However, broad classes of problems in science and engineering are amenable to a variational formulation as *minimum problems*, i. e., the physical states of interest minimize a certain energy functional. This variational characterization is meaningful regardless of the linear or nonlinear structure of the problem and does not presuppose a linear–much less normed–structure of the space of solutions (cf, e. g., [4] for modern accounts). Whereas in some cases the energy functional to be minimized is evident, in other cases the identification of the governing functional requires careful elucidation. For instance, in inelastic problems and dynamical problems minimum principles can be obtained by careful time discretization ([5–8]). In these cases the energy functional is incremental and encodes both the free energy, inertia and kinetics of the material.

In problems having a variational structure, the overriding criterion that governs every aspect of the system is energy minimization. Therefore, it is natural to allow the variational principle to drive mesh adaption as well. The concept of using the underlying variational principle to optimize the discretization enjoys a long tradition dating back, at least, to [9, 10], in the special context of two-dimensional linearized elasticity. When applied to the optimal placement of the nodes, or r-adaptivity, variational adaptivity is closely connected to configurational force balance ([11, 12]), a connection that has been recognized only recently [13–19].

In this paper we are concerned with the formulation of *variational h-adaption strategies* in which the variational principle itself drives mesh refinement and unrefinement. In particular, no error estimates are invoked at any stage of the adaption procedure. For definiteness, we confine our attention to simplicial meshes and edge bisection (cf [20–22]) as the device for achieving mesh refinement. Starting from a triangulation of the domain, the repeated application of edge bisection operations defines a *net* V_h of linear spaces parameterized by a *directed* index set A. The fundamental problem is then that of finding the absolute minimizers of the energy in the collection of spaces $\{V_h, h \in A\}$. However, this problem has combinatorial complexity and is intractable in general. Instead, we seek to identify *local minimizers*, i. e., minimizers that are stable with respect to a single edge bisection. The basic strategy that we adopt in order to arrive at local minimizers is to estimate the energy released by the bisection of each edge in the mesh; and to select for bisection the edge that results in the largest energy release, provided that this energy release is greater than a certain tolerance. This tolerance may be interpreted as the cost of introducing a new node in the mesh, expressed in units of energy. Evidently, the algorithm terminates when this cost is in excess of the energy release resulting from the bisection of every edge in the mesh.

Numerical tests show that this variational h-adaption strategy results in highly anisotropic and directional meshes that are sensitive to the gradients in the energy-density field. In particular, the variational h-adaption strategy results in highly elongated or flattened elements that are oriented so as to supply differing degrees of spatial resolution in different directions. Attempts to constrain this type of behavior, e. g., with a view to maintaining a certain upper bound on the aspect ratio of the elements of the mesh, are found to greatly diminish the performance of the adaption procedure measured, e. g., in terms of convergence rates. For instance, when the variational h-adaption is combined with RIVARA's longest-edge propagation path (LEPP) bisection algorithm [20–23], which guarantees an upper bound on the element aspect ratio, a marked performance degradation is recorded. Variational h-adaptivity can be coupled synergistically to variational r-adaption strategies in order to further improve performance.

The structure of the article is as follows. In Section 2, we start by briefly reviewing two representative classes of problems, finite elasticity and viscoplasticity, and their variational formulations, which provide context for subsequent developments. Variational h-adaptivity based on edge bisection and local configurational stability is introduced in Section 3. Finally, in Sec-

tion 4 we present three numerical examples that demonstrate the range and efficiency of the approach.

2 MODEL PROBLEMS

The fundamental concept behind variational adaptivity is to rely on the governing variational principle for purposes of optimizing the discretization. Therefore, the approach is dependent on existence of a variational–preferably a minimum–principle that characterizes the solutions of interest. For conservative systems such as hyperelastic bodies in static equilibrium, the attendant minimum principle is well-known. In other cases, including dynamical systems and dissipative solids, the existence of an underlying minimum principle is not obvious and its determination is in itself a matter of considerable interest. For purposes of illustration, we consider two classes of solids: hyperelastic solids governed by the principle of minimum potential energy; and isothermal viscoplastic solids governed by time-discretized incremental minimum principles. For completeness and subsequent reference, in this section we briefly summarize the formulation of the attendant variational problems.

2.1 Prototype problem I: Hyperelasticity

As an example of conservative system we consider an elastic solid occupying a domain $\Omega \in \mathbb{R}^3$ in its reference undeformed configuration and undergoing quasistatic deformations under the action of applied loads and displacement boundary conditions. The deformation mapping $\boldsymbol{\varphi}$ maps a particle $\boldsymbol{X} \in \Omega$ to its deformed position $\boldsymbol{x} \in \boldsymbol{\varphi}(\Omega)$. Locally, this deformation is measured by the deformation gradient $\boldsymbol{F} := \partial\boldsymbol{\varphi}/\partial\boldsymbol{X}$, which is subject to the local invertibility condition $J := \det \boldsymbol{F} > 0$. On the displacement boundary $\partial\Omega_1 \subset \Omega$, the deformation mapping is required to take the prescribed value $\bar{\boldsymbol{\varphi}}$, i. e.,

$$\boldsymbol{\varphi} = \bar{\boldsymbol{\varphi}}, \qquad \text{on } \partial\Omega_1\,. \tag{1}$$

By postulating a strain-energy density of the type $W(\boldsymbol{F})$, the first PIOLA-KIRCHHOFF stress tensor follows as

$$\boldsymbol{P} = \frac{\partial W(\boldsymbol{F})}{\partial \boldsymbol{F}}, \qquad \text{in } \Omega\,. \tag{2}$$

In the interior of Ω, $\boldsymbol{P}$ is required to be in equilibrium, i. e.,

$$\mathrm{DIV}\boldsymbol{P} + \boldsymbol{B} = \boldsymbol{0}, \qquad \text{in } \Omega\,, \tag{3}$$

where $\boldsymbol{B}$ denotes a body force field. Additionally, the stresses must be in equilibrium with the tractions $\bar{\boldsymbol{T}}$ applied on the traction boundary $\partial\Omega_2$, i. e.,

$$\boldsymbol{P}\cdot\boldsymbol{N} = \bar{\boldsymbol{T}}, \qquad \text{on } \partial\Omega_2\,, \tag{4}$$

where $\boldsymbol{N}$ is the normal outward vector to the boundary. The applied tractions $\bar{\boldsymbol{T}}$ and body forces $\boldsymbol{B}$ are assumed to be conservative. For definiteness, we restrict attention to the case of dead loading. Under these conditions, the potential energy of the body is

$$I(\boldsymbol{\varphi}) := \int_\Omega W(\mathrm{GRAD}\boldsymbol{\varphi})\,\mathrm{d}V - \int_\Omega \boldsymbol{B}\cdot\boldsymbol{\varphi}\,\mathrm{d}V - \int_{\partial\Omega_2} \bar{\boldsymbol{T}}\cdot\boldsymbol{\varphi}\,\mathrm{d}A\,. \tag{5}$$

The fundamental problem addressed in this work concerns the determination of the energy-minimizing configurations of the elastic body, which are presumed to represent the configurations at which the body is in stable equilibrium. The variational problem corresponding to this principle of minimum potential energy is:

$$\begin{array}{c} \inf \quad I(\boldsymbol{\varphi}) \\ \boldsymbol{\varphi} \in V, \\ \boldsymbol{\varphi}|_{\partial\Omega_1} = \bar{\boldsymbol{\varphi}} \end{array} \tag{6}$$

where V is some suitable configuration or solution space containing all the physically attainable possible deformations of the body.

The principle of minimum potential energy provides an unambiguous comparison criterion for test functions: a test function $\boldsymbol{\varphi}^{(1)}$ is *better* than another $\boldsymbol{\varphi}^{(2)}$ if *and only if* $I(\boldsymbol{\varphi}^{(1)}) < I(\boldsymbol{\varphi}^{(2)})$. All other considerations are, in effect, spurious. This energy comparison criterion is the basis of variational mesh adaption. It bears emphasis that the variational approach entirely eliminates the need for error estimation as a basis for adaptivity. This is particularly important in application areas, such as hyperelasticity, in which error estimates are not available or simply fail to make mathematical sense due to non-attainment, lack of uniqueness of the minimizers or non-metrizable solution spaces.

2.2 Prototype problem II: Variational formulation of viscoplastic constitutive updates

A broad class of constitutive models for dissipative materials are defined in terms of two scalar functions: an energy density function and a kinetic potential. Ortiz *et al.* ([5, 6]) have shown that the initial boundary-value problem associated with a broad class of those dissipative solids can be given a variational structure by recourse to time discretization. More precisely, the solutions of the time-discretized incremental problem are characterized by a minimum principle similar in structure to the principle of minimum potential energy. The requisite effective energy density $W_n(\boldsymbol{F}_{n+1})$ follows from a local relaxation of the internal state. Here, the subindex n refers to the discrete times t_n at which the solution is sampled, and the notation is intended to emphasize that the effective energy density W_n varies between time steps, thus allowing for irreversibility, hysteresis and dissipation. The fundamental property of the effective energy density is that it supplies a potential for the incremental stress-deformation relations, i. e.,

$$\boldsymbol{P}_{n+1} = \frac{\partial W_n}{\partial \boldsymbol{F}_{n+1}}(\boldsymbol{F}_{n+1}) \tag{7}$$

Similarly to hyperelasticity, the existence of an effective energy density allows the introduction of the incremental potential energy

$$I_n(\boldsymbol{\varphi}_{n+1}) := \int_\Omega W_n(\mathrm{GRAD}\boldsymbol{\varphi}_{n+1})\,\mathrm{d}V - \int_\Omega \boldsymbol{B}_{n+1}\cdot\boldsymbol{\varphi}_{n+1}\,\mathrm{d}V - \int_{\partial\Omega_2} \bar{\boldsymbol{T}}_{n+1}\cdot\boldsymbol{\varphi}_{n+1}\,\mathrm{d}A\,. \tag{8}$$

and the stable configurations of the solid at time t_{n+1} follow from the minimum principle

$$\begin{array}{c} \inf \quad I_n(\boldsymbol{\varphi}_{n+1}) \\ \boldsymbol{\varphi}_{n+1} \in V, \\ \boldsymbol{\varphi}_{n+1}|_{\partial\Omega_1} = \bar{\boldsymbol{\varphi}}_{n+1} \end{array} \tag{9}$$

For further details on the variational elastoplastic constitutive update, refer to Remark 1.

As in the case of hyperelasticity, this minimum principle provides an unambiguous comparison criterion for test functions: a test function $\boldsymbol{\varphi}_{n+1}^{(1)}$ is *better* than another $\boldsymbol{\varphi}_{n+1}^{(2)}$ if *and only if* $I_n(\boldsymbol{\varphi}_{n+1}^{(1)}) < I_n(\boldsymbol{\varphi}_{n+1}^{(2)})$. This comparison criterion in turn provides a suitable basis for variational adaptivity in problems involving dissipative materials.

Remark 1. Further details on variational constitutive updates can be found in [5, 6]. See also the more recent elaborations [24, 25]. A comparison between different variational updates is given in [26].

The specific model used in the numerical examples in this paper is based on a Helmholtz free energy functional of the type

$$W(\boldsymbol{F}, \boldsymbol{F}^{\mathrm{p}}, \varepsilon^{\mathrm{p}}) = W^{\mathrm{e}}(\boldsymbol{F} \cdot \boldsymbol{F}^{\mathrm{p}^{-1}}) + W^{\mathrm{p}}(\varepsilon^{\mathrm{p}}) \tag{10}$$

Here, W^{e} denotes the elastic free energy and W^{p} represents the stored energy due to plastic working of the material. According to Eq. (10), isotropic hardening has been assumed. In the computations presented in this paper, a Hencky-type model is adopted for W^{e} and a power-law hardening is employed for W^{p}.

While in conventional plasticity models, an admissible stress space is usually the primitive postulate of the theory and the flow rule is a derived law, the flow rule is the primitive postulate and the yield criterion is the derived law within the variational approach by Ortiz *et al.*, cf. [5, 6]. For example, in the case of von Mises plasticity theory, the following evolution equations are postulated a priori

$$\dot{\boldsymbol{F}}^{\mathrm{p}} \cdot \boldsymbol{F}^{\mathrm{p}^{-1}} = \dot{\varepsilon}^{\mathrm{p}}\, \boldsymbol{M}, \quad \mathrm{tr}(\boldsymbol{M}) = 0, \quad \frac{2}{3}\, \boldsymbol{M} : \boldsymbol{M} = 1, \quad \dot{\varepsilon}^{\mathrm{p}} \geq 0 \tag{11}$$

Eqs. (10) and (11) define the constitutive model applied in the numerical examples of this paper. Following [5, 6] and neglecting viscosity and rate effects, the incremental potential W_n in Eqs. (7) and (8) results from the minimization problem

$$W_n(\boldsymbol{F}) = \inf_{\boldsymbol{F}^{\mathrm{p}}_{n+1}, \varepsilon^{\mathrm{p}}_{n+1}} \left\{ W(\boldsymbol{F}, \boldsymbol{F}^{\mathrm{p}}_{n+1}, \varepsilon^{\mathrm{p}}_{n+1}) \right\} \tag{12}$$

subject to the discretized evolution Eqs. (11). Here, $(\bullet)_{n+1}$ denotes the variable $(\bullet)$ at time $n+1$ obtained by applying a time discretization.

3 VARIATIONAL h-ADAPTION

Variational h-adaption relies on the underlying variational principle to drive the process of mesh refinement and unrefinement. In particular, no error estimates are invoked at any stage of the adaption procedure. In this work we confine our attention to simplicial meshes and edge bisection (cf [20–22]) as the device for achieving mesh refinement, Fig. 1.

3.1 Variational edge-bisection criteria

Within a variational framework, the standard displacement finite-element method may be regarded as constrained minimization, with solutions restricted to a finite-dimensional subspace V_h of V. The constrained functional is

$$I_h(\boldsymbol{\varphi}) = \begin{cases} I(\boldsymbol{\varphi}), & \text{if } \boldsymbol{\varphi} \in V \\ +\infty, & \text{otherwise} \end{cases} \tag{13}$$

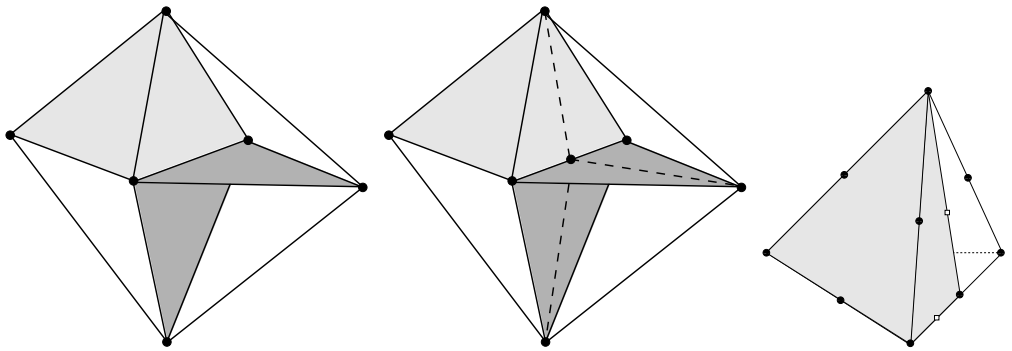

(a) (b) (c)

Figure 1: Edge-bisection of simplicial mesh. a) Edge star before bisection. b) Bisection and reconstruction of the star of the bisected edge. c) Edge bisection in a 10-node tetrahedral element by using edge bisection. The filled circles represent nodes existing prior to bisection; open squares indicate new nodes inserted as a result of bisection.

and the reduced problem is

$$\begin{array}{c} \inf \\ \boldsymbol{\varphi} \in V, \\ \boldsymbol{\varphi}|_{\partial\Omega_1} = \bar{\boldsymbol{\varphi}} \end{array} \quad I_h(\boldsymbol{\varphi}) \tag{14}$$

The subspaces V_h are generated by introducing a triangulation $\mathcal{T}_h$ of Ω and a standard finite element interpolation of the form

$$\boldsymbol{\varphi}_h(\boldsymbol{X}) = \sum_{a=1}^{N_h} \boldsymbol{x}_a N_a(\boldsymbol{X}) \tag{15}$$

where N_h is the number of nodes, N_a denotes the nodal shape function of node a and $\boldsymbol{x}_a$ is the nodal position vector in the deformed configuration. Classically, one regards V_h as a sequence of subspaces parameterized, e. g., by the mesh size h, and seeks a sequence $\boldsymbol{\varphi}_h$ of approximate solutions such that $I_h(\boldsymbol{\varphi}_h) \to I(\boldsymbol{\varphi})$.

Suppose instead that V_h represents a *net* of linear spaces parameterized by a *directed* index set A. Recall that a directed set is a set A together with a binary relation $\leq$ having the following properties: i) $a \leq a$ for all $a \in A$ (reflexivity); if $a \leq b$ and $b \leq c$, then $a \leq c$ (transitivity); for any pair $a, b \in A$, there exists $c \in A$ such that $a \leq c$ and $b \leq c$ (directedness). In the present work, we consider nets of subspaces generated by *edge bisection*. Thus, $V_{h_1} \leq V_{h_2}$ if the triangulation $\mathcal{T}_{h_2}$ corresponding to V_{h_2} can be reached from the triangulation $\mathcal{T}_{h_1}$ corresponding to V_{h_1} by a sequence of edge bisections. In addition, we shall suppose that there is an element $0 \in A$ that precedes all other elements. The corresponding triangulation $\mathcal{T}_0$ is the initial mesh, and V_0 is the corresponding initial solution space.

As noted earlier, the variational principle supplies an unambiguous comparison criterion for judging the relative quality of two test functions: $\boldsymbol{\varphi}_{h_2}$ is *better* than $\boldsymbol{\varphi}_{h_1}$ if *and only if* $I(\boldsymbol{\varphi}_{h_2}) < I(\boldsymbol{\varphi}_{h_1})$. Hence, the problem of variational mesh adaption can be formulated as the minimum problem

$$\begin{array}{c} \inf \\ \boldsymbol{\varphi} \in V, \\ \boldsymbol{\varphi}|_{\partial\Omega_1} = \bar{\boldsymbol{\varphi}}, \\ h \in A \end{array} \quad I_h(\boldsymbol{\varphi}) + \mu_c N_h \tag{16}$$

where N_h denotes the number of nodes in the triangulation $\mathcal{T}_h$ and $\mu_c > 0$ is an *energy tolerance*. Evidently, μ_c represents the energy *cost* of introducing an additional node in the mesh and,

therefore, may be regarded as a *chemical potential*. The role played by the second term in (16) is to assign a cost μ_c to the introduction of an additional node. This cost in turn sets an upper limit to the size of the mesh. Thus, if $\mu_c = 0$ minimization of I_h results in run-away meshes, since the energy is always lowered by the introduction of additional nodes. By way of contrast, suppose that $\mu_c > 0$ and that the initial triangulation $\mathcal{T}_0$ is coarse, so that the minimizer V_0-minimizer is not a solution of (16). Then, as convergence is approached the addition of nodes results in diminishing energy returns and the second term in (16) is expected to dominate, with the result that the process of mesh refinement is eventually held in check.

The problem (16) of finding absolute minimizers in the collection of spaces $\{V_h, h \in A\}$ is of combinatorial complexity and, therefore, intractable in general. Instead, we shall be content with identifying *local minimizers*, i. e., minimizers that are stable with respect to a single edge bisection. In order to formalize this notion, let $E(\mathcal{T}_h)$ denote the collection of edges of $\mathcal{T}_h$. In addition, for all $e \in E(\mathcal{T}_h)$ let $\sigma_e : A \to A$ denote a mapping such that $\mathcal{T}_{\sigma_e(h)}$ is the triangulation resulting from the bisection of e. Then, we shall say that $\mathcal{T}_h$ is *bisection-stable* if

$$\mu(\mathcal{T}_h) = \max_{e \in E(\mathcal{T}_h)} \left(\inf I_h - \inf I_{\sigma_e(h)} \right) \leq \mu_c. \tag{17}$$

Thus, $\mathcal{T}_h$ is bisection-stable, the addition of one node lowers I_h at best by an amount $\mu(\mathcal{T}_h)$ less than μ_c, and thus the addition is to be rejected. The basic h-refinement strategy that emerges from these considerations may be summarized as follows:

i) Initialize $h = 0$.

ii) Find $e \in E(\mathcal{T}_h)$ for which $\mu(\mathcal{T}_h)$ is attained.

ii) Is $\mu(\mathcal{T}_h) > \mu_c$

YES: Reset $h \leftarrow \sigma_e(h)$, GOTO (ii).

NO: EXIT.

Remark 2. Instead of bisecting single edges sequentially, alternative strategies may be devised by ordering the supercritical edges according to the indicator $\inf I_h - \inf I_{\sigma_e(h)}$ and targeting for bisection a subset of those edges. Additionally, if the aspect ratio of the elements needs to be maintained, edges can be bisected by means of RIVARA's longest-edge propagation path (LEPP) bisection algorithm [20–23], which guarantees an upper bound on the element aspect ratio. However, it should be noted that in a strict variational framework aspect ratio is a poor measure of mesh quality. Indeed, as will become evident from the subsequent examples energy minimization often selects for strongly anisotropic meshes.

Remark 3. Higher-order elements, such as 10-node quadratic tetrahedra are commonly implemented by recourse to Gaussian quadrature. This introduces bounded errors that do not affect convergence in general. However, it should be noted that some of the strict ordering of energies implied by the variational structure of the problems may be lost due to numerical quadrature errors.

Remark 4. For linear systems the potential energy has the representation:

$$I(v) = \frac{1}{2} a(v, v) - l(v) \tag{18}$$

where $a(v,v)$ is a quadratic form and $l(v)$ a bounded linear functional. Suppose that $a(v,v)$ is coercive and bounded in the V-norm. Then, $I(v)$ has a unique minimizer u and we have the identity

$$I(v) = \frac{1}{2}a(v-u, v-u) - \frac{1}{2}a(u,u) \tag{19}$$

Evidently, under these conditions minimization of $I(v)$ is equivalent to minimizing the energy-norm error $||v-u||_E = \sqrt{a(v-u, v-u)}$. In particular, the effect of variational mesh-adaption is to minimize the energy-norm error.

Remark 5. It should be carefully noted that the functional framework just outlined does not carry over to general nonlinear problems. For instance, in problems such as finite elasticity it is natural to resort to weak topologies, with the result that the solution space is not a normed space. Furthermore, if geometrical constraints such as local invertibility of the deformations are appended, the solution space is not even a linear space. Finally, the minimizers are *a fortiriori* non-unique by virtue of geometrical instabilities such as buckling or material instabilities such as twinning. Under these conditions the notion of *error*, defined as the norm distance between approximate solutions and a unique minimizer, fails to apply.

Remark 6. The variational principle can also be taken as a basis for driving *mesh coarsening* or *unrefinement* in addition to refinement. A common technique for mesh coarsening is edge collapse (see, e. g., [27, 28]). In the present context, an appealing alternative is to record each edge bisection so that it can be subsequently *reversed*. However, these extensions of the method will not be considered here.

3.2 Bisection criteria derived from local energy bounds

Evidently, a drawback of the strategy just outlined is that the energy $\mu(\mathcal{T}_h)$ released by bisection is costly to compute exactly. An alternative strategy consists of working with a lower bound of $\mu(\mathcal{T}_h)$. A convenient such lower bound can be obtained by constraining the relaxation of the displacement field upon bisection of an edge e to a certain sub-mesh $\mathcal{S}_h(e)$ of $\mathcal{T}_h$, or element *patch*, containing e. For instance, $\mathcal{S}_h(e)$ can be set to the ring of elements incident to e, i. e., the *star* $\mathrm{St}(e)$. Evidently,

$$\mu_{\mathrm{loc}}(\mathcal{T}_h) = \max_{e\in E(\mathcal{T}_h)} \left\{ I_h(\boldsymbol{\varphi}_h) - \inf_{\substack{\boldsymbol{\varphi}\in V,\\ \boldsymbol{\varphi}|_{\partial\Omega_1}=\bar{\boldsymbol{\varphi}},\\ \mathrm{supp}(\boldsymbol{\varphi}-\boldsymbol{\varphi}_h)\subset\mathcal{S}_h(e)}} I_{\sigma_e(h)}(\boldsymbol{\varphi}) \right\} < \mu(\mathcal{T}_h) \tag{20}$$

supplies the requisite lower bound. In this expression, φ_h is minimizer of I_h and supp denotes the support of a function. Thus, $\mu_{\mathrm{loc}}(\mathcal{T}_h)$ is computed by constraining the relaxed displacements $\boldsymbol{\varphi}$ on the bisected mesh $\mathcal{T}_{\sigma_e(h)}$ to differ from the minimizer $\boldsymbol{\varphi}_h$ on the un-bisected mesh $\mathcal{T}_h$ only within the neighborhood $\mathcal{S}_h(e)$ of the bisected edge e. Conveniently, this computation is local and its cost is constant independent of the size of the mesh. The resulting h-adaption strategy is:

i) Initialize $h = 0$.

ii) Find $e \in E(\mathcal{T}_h)$ for which $\mu_{\mathrm{loc}}(\mathcal{T}_h)$ is attained.

ii) Is $\mu_{\mathrm{loc}}(\mathcal{T}_h) > \mu_c$

YES: Reset $h \leftarrow \sigma_e(h)$, GOTO (ii).

NO: EXIT.

Remark 7. Locally constrained problems such as defined have also been proposed as a basis for deriving *a posteriori* error bounds in linear problems [1, 2].

Remark 8. Because of the lower bound property $\mu_{\rm loc}(\mathcal{T}_h) < \mu_{\rm loc}$, the adaption strategy based on the local estimate $\mu_{\rm loc}(\mathcal{T}_h)$ may be expected to accept meshes that would otherwise be bisection-unstable according to the global energy criterion.

Remark 9. When dealing with constant-strain elements, the case of boundary edges connected to one single element, henceforth referred to as *sharp edges*, may require special handling. For sharp edges, the local patch $\mathcal{S}_h(e)$ consists of one single constant-strain element in the special case in which the local patch is taken to coincide with the star of the edge, $\mathcal{S}_h(e) = \mathrm{St}(e)$. Under these conditions, bisection of a sharp edge leaves the energy invariant, with the result that sharp edges are never targeted for bisection. In order to avoid this artifact the local patches of sharp edges need to be extended beyond their stars.

Remark 10. The problem of sharp edges alluded to in Remark 9 does not arise when higher-order elements, such as 10-node quadratic tetrahedra, are in use.

Remark 11. Variational r-adaption relies on energy minimization in order to determine the optimal location of the nodes and the connectivity of the mesh [13, 16, 17, 19]. In principle, variational r- and h-adaption can be combined sequentially to obtain a variational $h-r$ adaption strategy. A limited application of variational r-adaption in the context of variational h-adaption is for purposes of optimizing the location of the new nodes inserted by bisection. Conveniently, when local energy estimates are utilized the r-optimization can also be performed locally in combination with the solution of problem (20).

4 NUMERICAL EXAMPLES

We proceed to demonstrate the performance of variational h-adaption by means of selected tests including: a notched specimen in uniaxial tension; the indentation of a hyperelastic block; and the indentation of an elastic-plastic block. One clear performance measure of primary importance is the rate of convergence. Specifically, we wish to ascertain whether–and if so, to what extent–variational h-adaption accelerates convergence in energy. An additional central question concerns the characterization of the mesh geometries that are energetically optimal. A common rule-of-thumb is to assume that the quality of an element is commensurate with its aspect ratio, defined as the ratio between the outer and inner radii of the element. However, the aspect ratio enters error estimates as a direct consequence of the use of matrix-norm bounds that are isotropic in nature and, consequently, not tight in general. In particular, those estimates are insensitive to the directionality of the gradients in the error function. Aspect ratio bounds can be maintained throughout the mesh refinement process, e. g., by recourse to RIVARA's longest-edge propagation path (LEPP) bisection algorithm [20–23]. Therefore, we wish to ascertain whether appending constraints on the aspect ratio of the elements speeds up or slows down convergence.

4.1 Uniaxial tensile test of a notched specimen

Our first test case concerns a hyperelastic three-dimensional notched specimen undergoing large deformations in uniaxial tension, Fig. 2. In view of the symmetries of the problem the calculations are conveniently restricted to one eighth of the specimen (see Fig. 3a). The material is

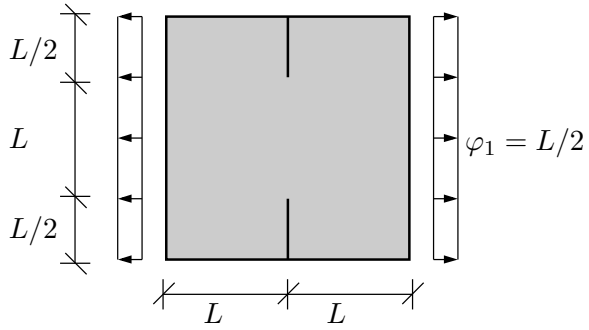

Figure 2: Geometry of the hyperelastic three-dimensional notched specimen undergoing large deformations in uniaxial tension. The size of the specimen is $L = 2.0$ m. The depth of the specimen is L.

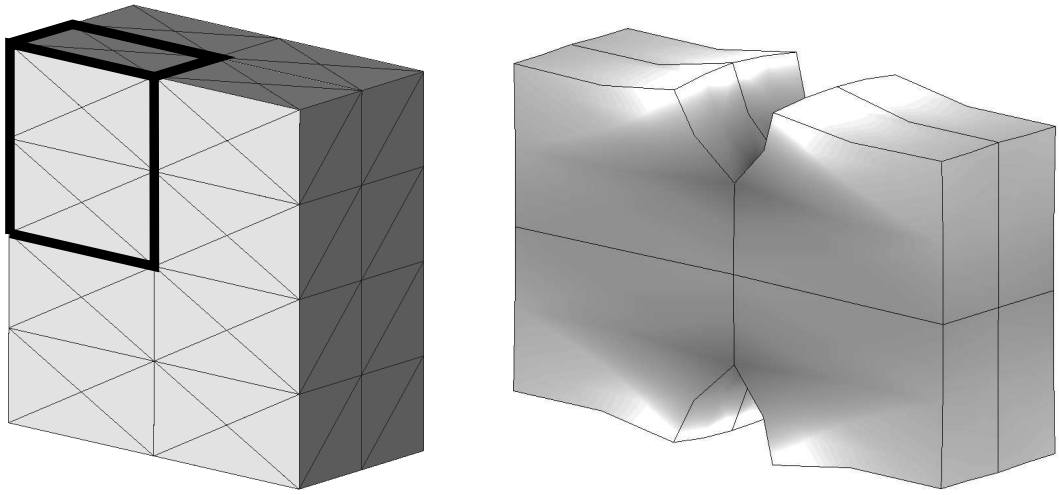

(a) (b)

Figure 3: Geometry of the hyperelastic three-dimensional notched specimen undergoing large deformations in uniaxial tension. a) initial discretization; the octant of the specimen considered in the calculations is highlighted. b) deformed body and stored-energy distribution, showing concentration at the crack tips and nearly uniform variation across the specimen.

hyperelastic with energy density

$$W(\boldsymbol{F}) = \frac{1}{2}\,\lambda\,\ln^2 J + \frac{1}{2}\,\mu\,\left[\boldsymbol{F}:\boldsymbol{F} - 3 - 2\,\ln J\right], \qquad J := \det \boldsymbol{F} \tag{21}$$

The LAMÉ constants are: $\lambda = 12115.38$ N/m^2 and $\mu = 8071.92$N/m^2.

The response of the specimen is baselined by means of a coarse discretization consisting of 10-node quadratic tetrahedral elements. The corresponding finite element mesh, deformation and the stored energy distribution are shown in Fig. 3. As expected, the energy density attains its maximum in the vicinity of the crack tip; and is nearly uniform in the thickness direction of the slab.

Figs. 4 and 5 show the results of two adaptive calculations: an unconstrained variational h-adaption calculation, in which only the energetically most favorable edge is bisected at each step; and a constrained variational h-adaption calculation, in which an upper bound on the aspect ratio of the elements is maintained by means of RIVARA's longest-edge propagation path

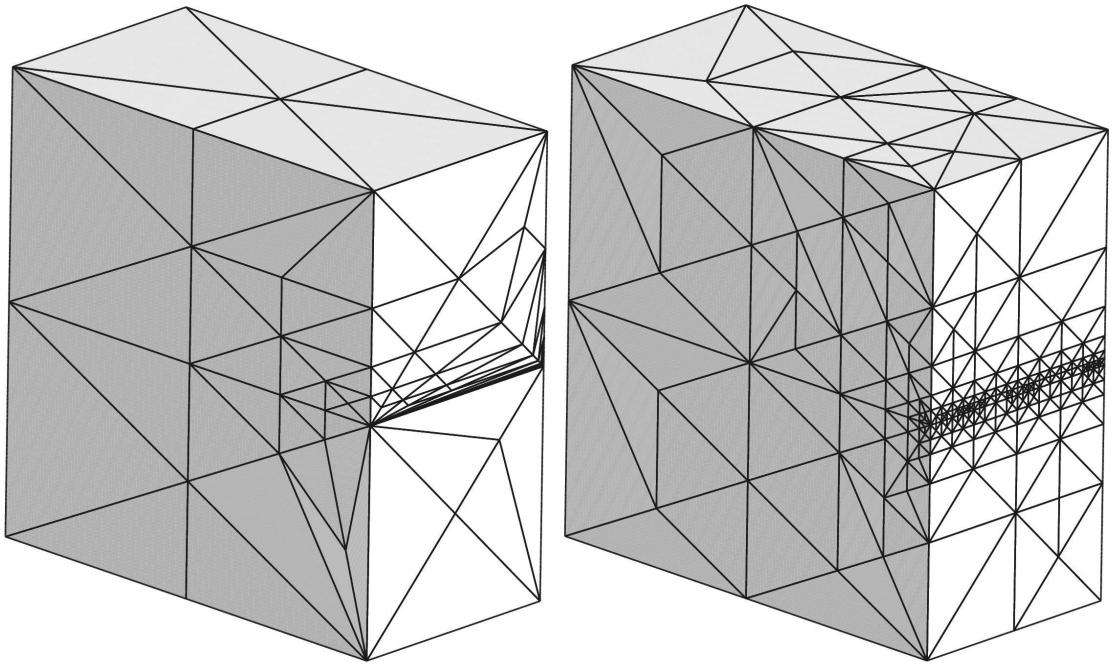

(a) (b)

Figure 4: Hyperelastic three-dimensional notched specimen undergoing large deformations in uniaxial tension. Final mesh geometries resulting from: a) Unconstrained variational h-adaption, showing anisotropic mesh refinement at the tip. b) Constrained variational h-adaption using RIVARA's LEPP algorithm showing isotropic mesh refinement at the tip.

(LEPP) bisection algorithm [20–23]. We recall that in the LEPP bisection algorithm the upper bound on the element aspect ratio is maintained by bisecting edges other than the target edge, in addition to bisecting the target edge itself. The final meshes obtained by the two procedures stand in sharp contrast to one another, Fig. 4. Thus, unconstrained variational h-adaption clearly allocates resources in such a way as to exploit the directionality of the gradients in the variation of the solution, Fig. 4a. In particular, it results in highly *anisotropic* mesh refinement: a high degree of mesh refinement in the directions normal to the crack tip; and simultaneously a nearly uniform mesh size in the direction of the crack tip from, i. e., across the thickness of the specimen. It bears emphasis that this anisotropic refinement occurs spontaneously as an energetic optimum, and is not the result of empirical criteria built into the adaption strategy. By way of contrast, the constrained variational h-adaption calculation results in *isotropic* mesh refinement, with equi-axed elements distributed through the thickness of the specimen, Fig. 4b. The convergence rates in energy of the constrained and unconstrained variational h-adaption calculations are compared in Fig. 5 with the convergence rate resulting from uniform refinement. We note that, in the linear range, the energy error plotted in the ordinate reduces to: $a(u_h, u_h) - a(u, u) = a(u_h - u, u_h - u) = ||u_h - u||^2_E$, and hence may be thought of as generalizing the conventional energy-norm error to the nonlinear range. Clearly, the performance of unconstrained variational h-adaption is superior to that of constrained variational h-adaption. In particular, anisotropic mesh refinement results in higher convergence rates than isotropic mesh refinement. Thus, far from being detrimental, highly-elongated elements oriented according to the gradients in the solution are beneficial to performance. Conversely, constraints designed to eliminate elongated elements, while resulting in meshes that are more 'pleasing to the eye', have a detrimental effect on the rate of convergence.

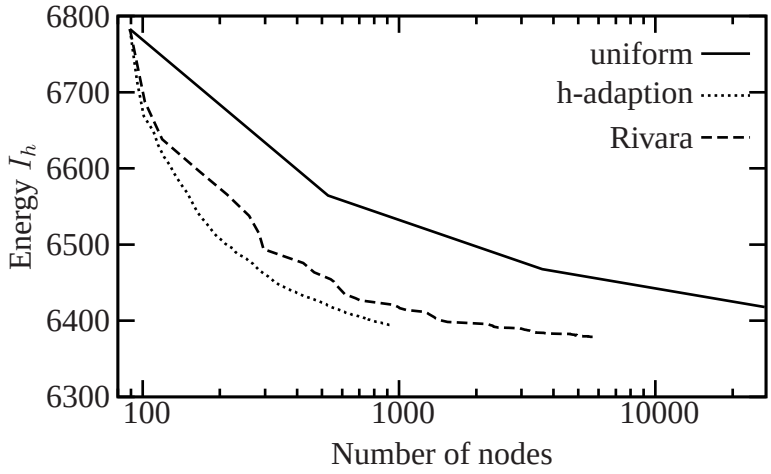

Figure 5: Hyperelastic three-dimensional notched specimen undergoing large deformations in uniaxial tension. Comparison of convergence rates resulting from unconstrained and constrained variational h-adaption. The convergence rate corresponding to uniform refinement is also shown for comparison.

4.2 Indentation of a hyperelastic block

We proceed to illustrate the performance of the coupled variational hr-adaption strategy. The test case concerns the indentation of a finitely-deforming hyperelastic block, Fig. 6. The block is indented by a rigid punch of circular cross section. Loading is effected by displacement control up to a maximum punch travel of 0.1 m. The energy density of the material is given in Eq. (21). We take advantage of the symmetries of the problem to restrict the calculations to a quarter of the specimen. The response predicted by the initial finite element mesh, consisting of 10-node quadratic tetrahedral elements, is shown in Fig. 7. As expected, the strain energy attains its maximum under the punch and exhibits power-law decay away from it, Fig. 7b. However, the region immediately under the punch is highly confined and is in a state of high triaxiality and comparatively lower energy. Owing to the concentration and fine structure of the strain energy, the problem lends itself ideally to mesh adaption.

Fig. 8 displays the final meshes obtained by means of three adaption strategies: unconstrained variational h-adaption; unconstrained variational hr-adaption; and constrained variational h-adaption using RIVARA's LEPP algorithm to maintain an upper bound on the aspect ratio of the elements. As remarked earlier, the variational hr-adaption procedure employed in the calculations consists of alternating edge bisection and the variational r-adaption scheme described in [19]. As in the case of the notched specimen described in the foregoing, the strain-energy distribution under punch exhibits not only concentration but also marked directionality. Thus, whereas the strain-energy displays rapid variation in the radial direction, it varies slowly in the orthogonal directions and, in particular, it is constant in the circumferential direction. As expected, the LEPP-constrained scheme results in an isotropic mesh that is insensitive to the directionality of the solution. In consequence, at any given depth of indentation it inserts a larger number of nodes than the remaining algorithms. By contrast, unconstrained h and hr-adaption results in highly anisotropic and directional meshes that trace the fine structure of the energy-density field.

Fig. 9 compares the energy convergence behavior of the three methods. As may be seen from this comparison, hr-adaptivity results in appreciable but modest gains in the rate of convergence relative to h-adaptivity. In addition, both h and hr-adaptivity handily out-perform constrained

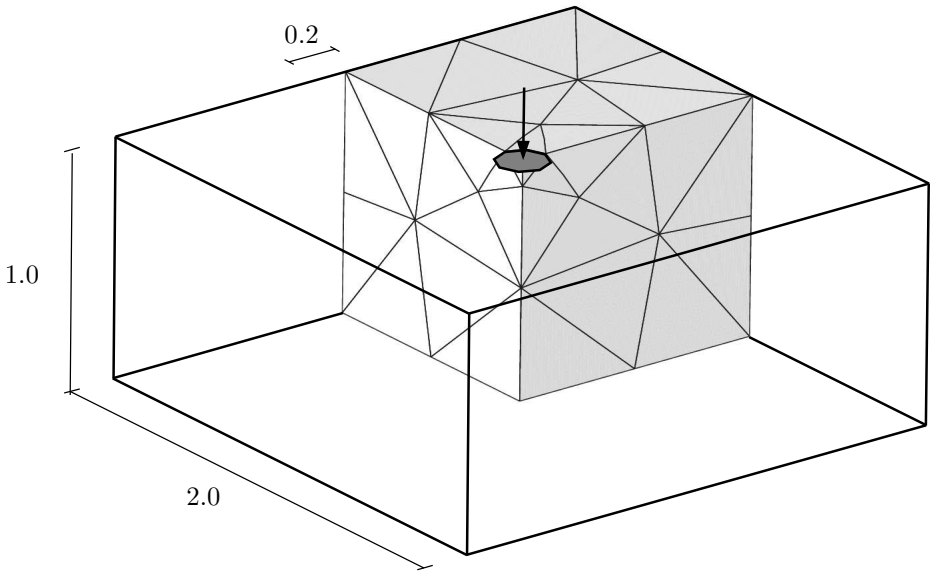

Figure 6: Indentation of a hyperelastic block by a circular rigid punch. Initial discretization

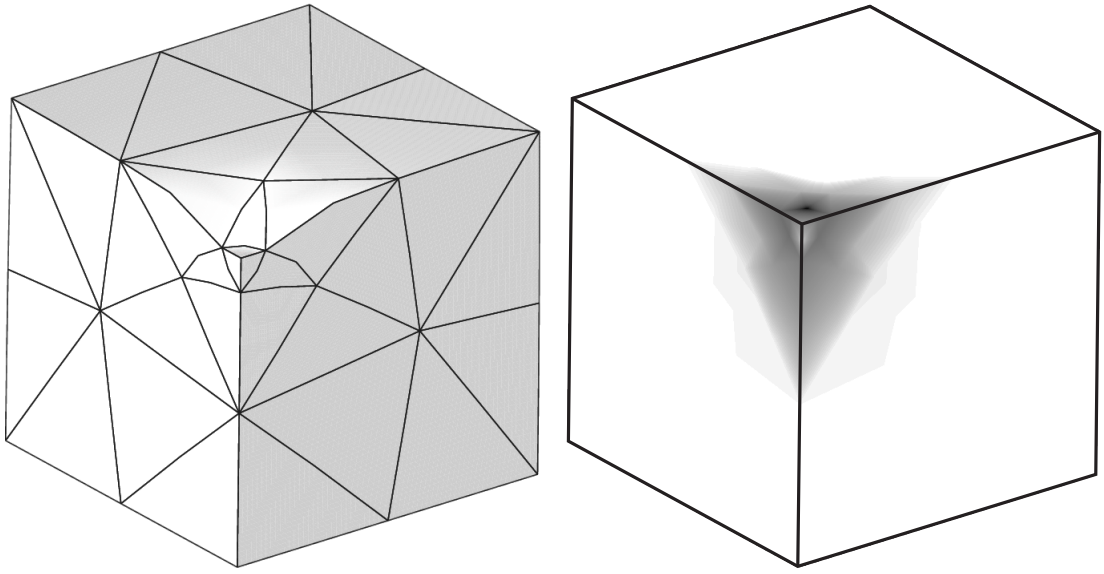

(a) (b)

Figure 7: Indentation of a hyperelastic block by a circular rigid punch, initial mesh. a) Deformed configuration. b) Stored-energy distribution.

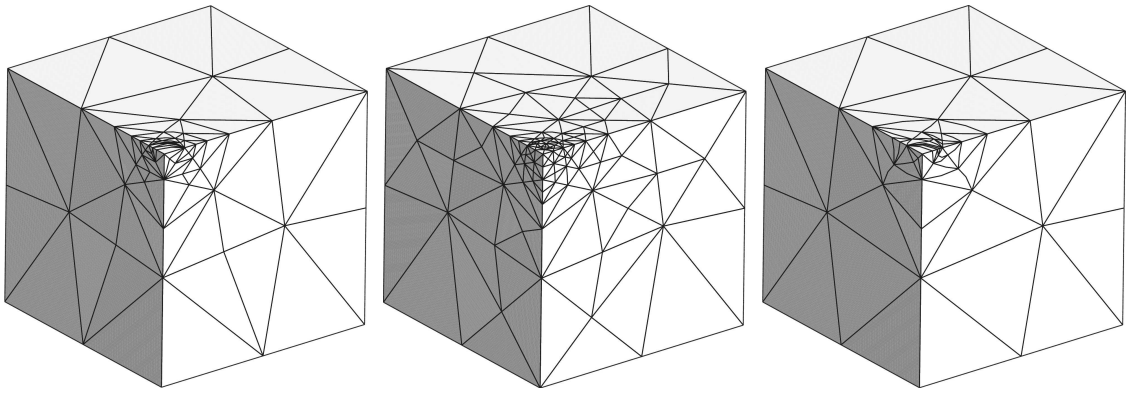

(a) (b) (c)

Figure 8: Indentation of a hyperelastic block by a circular rigid punch. Final meshes after: a) Unconstrained variational h-adaption. b) Constrained variational h-adaption using RIVARA's LEPP algorithm. c) Unconstrained variational hr-adaption.

h-adaptivity. For instance, a 676-node unconstrained h-adaption solution has lower energy than a uniformly refined discretization having 9721 nodes. If, in addition, r-adaption is allowed for the size of the mesh can be further reduced to 491 nodes at no increase in energy. These performance differentials, similar to those observed in the notched specimen example, provide compelling demonstration of the fact that element aspect ratio does not correlate well with performance in problems exhibiting strong directionality in the energy-density field.

4.3 Indentation of an elastic-plastic block

Finally, we demonstrate the applicability of the variational approach to inelastic materials by considering the problem of indentation of an elastic-plastic block by a rigid circular punch. The problem is identical in every way to that treated in the preceding section with the sole exception that the material is now assumed to obey multiplicative J_2-flow theory of plasticity. As discussed in Section 2.2, a time discretization using variational constitutive updates [5, 6] confers the incremental problem a variational structure identical to that of a hyperelastic problem. In particular, the deformation mapping at time t_{n+1} minimizes an incremental potential energy defined in terms of an effective strain-energy density that encodes both the elastic and the inelastic behavior of the material. In this setting, variational h-adaptivity consists of optimizing the mesh at every time step with respect to the incremental potential energy. In particular, for any given time step the variational h-adaptivity solution procedure is identical to that pertaining to an elastic problem.

The maximum depth of indentation considered in the calculations is of 0.02 m. All meshes consist of 10-node quadratic tetrahedral elements. For definiteness, in calculations we assume: Hencky-elastic behavior in terms of logarithmic elastic strains (e. g., [6, 29, 30]); rate-independent behavior; and power-law hardening of the form (cf, e. g., [6, 29])

$$W^{\mathrm{p}}(\varepsilon^{\mathrm{p}}) = \frac{n\sigma_0\varepsilon_0^{\mathrm{p}}}{n+1}\left[1+\left(\frac{\varepsilon^{\mathrm{p}}}{\varepsilon_0^{\mathrm{p}}}\right)\right]^{(n+1)/n} \tag{22}$$

where ε^{p} is the effective Mises plastic strain; σ_0 is a flow stress; $\varepsilon_0^{\mathrm{p}}$ is a reference effective plastic strain; and n is the hardening exponent. The material parameters used in calculations are summarized in Table 1. The state variables are assumed to be piecewise constant over the

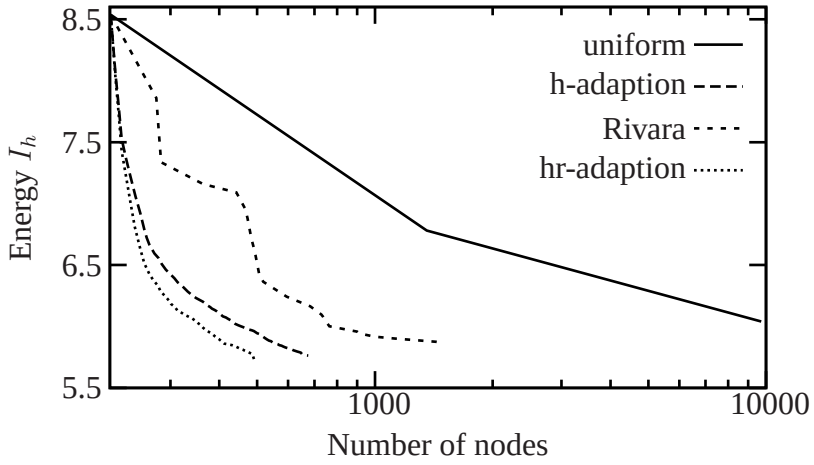

Figure 9: Indentation of a hyperelastic block by a circular rigid punch. Convergence in energy resulting from: unconstrained variational h-adaption; constrained variational h-adaption using RIVARA's LEPP algorithm; unconstrained variational hr-adaption; and uniform mesh refinement.

E (kN/m^2)	ν	σ_0 (kN/m^2)	$\varepsilon_0^{\mathrm{p}}$	n
200	0.2	1.0	$0.5 \cdot 10^{-3}$	10

Table 1: Indentation of an elastic-plastic block: material parameters

VORONOI cells defined by the quadrature points. Upon bisection, the internal variables are remapped to the new mesh by means of the variational transfer operator of [31]. By the use of piecewise-constant interpolation, the consistent transfer operator according to [31] simplifies greatly. More precisely, the history variables at a newly inserted GAUSS point equal those of the closest old quadrature point. As already mentioned in [5], this method guarantees that internal constraints such as $\det \boldsymbol{F}^{\mathrm{p}} = 1$ are preserved.

As in the previous examples, two different adaptive computations are performed: unconstrained variational h-adaption; and constrained variational h-adaption using RIVARA's LEPP algorithm to maintain an upper bound on the aspect ratio of the elements. In addition, two uniform refinement steps are evaluated by way of baseline. The distribution of the effective plastic strain ε^{p} is shown in Fig. 10. Fig. 10a shows a mesh generated by applying two uniform refinement steps to the initial discretization of Fig. 6. The meshes in Figs. 10b and c are the result of the unconstrained and constrained variational h-adaption schemes, respectively. As in the preceding examples, the contrast between the unconstrained and constrained adaption schemes is clearly evident in Figs. 10b and c. Thus, the unconstrained variational h-adaption strategy results in a highly anisotropic and localized mesh that is in sharp contrast to the isotropic and diffuse mesh produced by the constrained strategy. In particular, the unconstrained mesh traces a *slip cone* that separates the triaxial plug under the indentor from the matrix. The elements tiling the slip cone are flat and elongated, with the result that the entire slip-cone mechanism is represented with a modicum of degrees of freedom. The corresponding plastic strain field is highly localized to the slip cone, and elastic unloading occurs elsewhere. By way of contrast, the constrained plastic strain field is diffuse and does not show signs of localization. This excessive *numerical diffusion* effectively eliminates all traces of the slip cone and results in an artificially smooth plastic strain distribution.

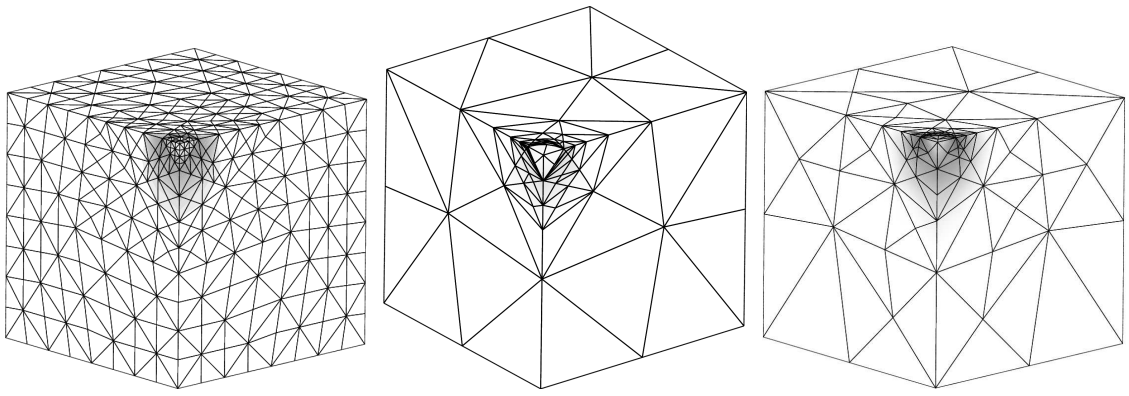

Figure 10: Indentation of an elastic-plastic block. Distribution of effective plastic strain ε^{p}. a) Two uniform refinement steps. b) Unconstrained h-adaption. c) Constrained h-adaption using RIVARA's LEPP algorithm.

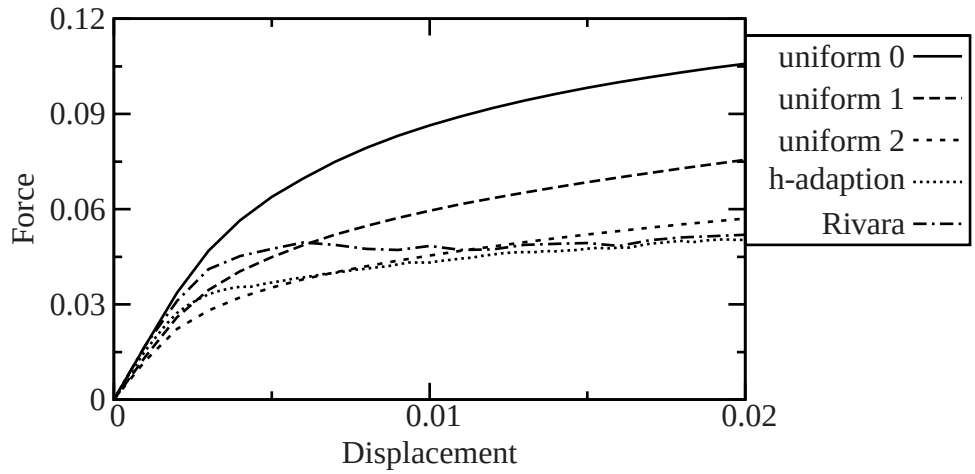

Figure 11: Indentation of an elastic-plastic block. Load-displacement diagrams obtained from: initial mesh (uniform 0); two uniform refinement steps (uniform 1 and 2); and variational h-adaption.

The various load-displacement diagrams are collected in Fig. 11 for ease of comparison. As expected, the coarse discretizations overestimate the indentation load and stiffness. Uniform refinement progressively relaxes the predicted response, but an overly stiff response remains even at the finest level of refinement. By contrast, the adaptive solutions predict a clear failure load, with the most compliant response corresponding to the unconstrained solution. However, a certain lag is observed initially in the adaptive solutions, which results from the gradual way in which refinement is introduced. Control over this lag can be exerted through the choice of energy tolerance μ_c.

5 SUMMARY AND CONCLUDING REMARKS

We have developed a variational h-adaption strategy in which the evolution of the mesh is driven directly by the governing minimum principle. This minimum principle varies according

to the physical nature of the problem, e. g., the principle of minimum potential energy in the case of elastostatics. In problems involving inelastic behavior minimum governing principles for the incremental static problem can be obtained by recourse to time discretization. Meshes are adapted by the recursive application of edge-bisection operations. In particular, an edge is bisected when the resulting energy or incremental pseudo-energy released exceeds a certain threshold value. In order to avoid global recomputes, we estimate the local energy released by mesh refinement by means of a lower bound obtained by relaxing a local patch of elements. This bound can be computed locally, which reduces the complexity of the refinement algorithm to $O(N)$. Variational h-refinement can be additionally combined with variational r-refinement to obtain a variational hr-refinement algorithm. Our numerical tests show that variationally adapted meshes are highly anisotropic and directional, and oriented themselves according to the gradients in the energy-density field. We also show that variational h-adaption outperforms other refinement strategies based on aspect ratio or other purely geometrical measures of mesh quality. The versatility and rate of convergence of the resulting approach has been demonstrated by means of selected numerical tests.

It is remarkable that anisotropic mesh refinement arises spontaneously, without recourse to empirical rules, as a result variational h adaption. The resulting elements, while optimal in an energy sense, are highly elongated or flattened, and supply varying degrees of spatial resolution in different directions. The ability to resolve sharp gradients in one direction without excessive mesh refinement in the remaining directions is of critical importance for dealing efficiently with features such as slip surfaces and shear bands. Indeed, in this cases isotropic mesh refinement inevitably leads to rapid growth of the problem size. More troubling yet, isotropic mesh adaption tends to be overly diffusive, thereby inhibiting strain localization and resulting in artificially smooth solutions. It is within this context, where purely geometrical element-quality measures fall short, that variational h-adaption is expected to be most effective.

ACKNOWLEDGMENT

Support from the DoE through Caltech's ASC/ASAP Center for the Simulation of the Dynamic Response of Solids is gratefully acknowledged. JM is also grateful for support from the Deutsche Forschungsgemeinschaft (DFG) under contract/grant number: Mo 1389/1-1.

References

[1] R. Verfürth. *A review of a priori error estimation and adaptive mesh-refinement techniques*. Wiley-Teubner, 1996.

[2] M. Ainsworth and J.T. Oden. *A Posterior Error Estimation in Finite Element Analysis*. Wiley, 2000.

[3] P. Ciarlet. *Mathematical elasticity. Volume I: Three-dimensional elasticity*. North-Holland Publishing Company, Amsterdam, 1988.

[4] B. Dacorogna. *Direct Methods in the Calculus of Variations*. Springer-Verlag, New York, 1989.

[5] R. Radovitzky and M. Ortiz. Error estimation and adaptive meshing in strongly nonlinear dynamic problems. *Computer Methods in Applied Mechanics and Engineering*, 172:203–240, 1999.

[6] M. Ortiz and L. Stainier. The variational formulation of viscoplastic constitutive updates. *Computer Methods in Applied Mechanics and Engineering*, 171:419–444, 1999.

[7] M. Ortiz and E.A. Repetto. Nonconvex energy minimisation and dislocation in ductile single crystals. *J. Mech. Phys. Solids*, 47:397–462, 1999.

[8] Q. Yang, L. Stainier, and M. Ortiz. A variational formulation of the coupled thermo-mechanical boundary-value problem for general dissipative solids. *Journal of the Mechanics and Physics of Solids*, 54:401–424, 2006.

[9] G.M. McNeice and P.V. Marcal. Optimization of finite-element grids based on minumum potential-energy. *Journal of Engineering for Industry-Transactions of the ASME*, 95(1):186–190, 1973.

[10] C. Felippa. Numerical experiments in finite element grid optimization by direct energy search. *Appl. Math. Modelling*, 1:93–96, 1976.

[11] J.D. Eshelby. The force on an elastic singularity. *Phil. Trans. R. Soc. Lond. A*, 244:87–112, 1951.

[12] J.D. Eshelby. The elastic energy-momentum tensor. *J. Elasticity*, 5:321–335, 1975.

[13] M. Braun. Configurational forces induced by finite element discretization,. *Proc. Estonian Acad. Sci. Phys. Math.*, 46:24–31, 1997.

[14] R. Mueller and G.A. Maugin. On material forces and finite element discretizations. *Computational Mechanics*, 29:52–60, 2002.

[15] P. Thoutireddy. *Variational Arbitrary Lagrangian-Eulerian method*. PhD thesis, California Institute of Technology, Pasadena, USA, 2003.

[16] P. Thoutireddy and M. Ortiz. A variational r-adaption and shape-optimization method for finite-deformation elasticity. *International Journal for Numerical Methods in Engineering*, 61:1–21, 2004.

[17] E. Kuhl, H. Askes, and P. Steinmann. An ALE formulation based on spatial and material settings of continuum mechanics. Part 1: Generic hyperelastic formulation. *Computer Methods in Applied Mechanics and Engineering*, 193(39-41):4207–4222, 2004.

[18] H. Askes, E. Kuhl, and P. Steinmann. An ALE formulation based on spatial and material settings of continuum mechanics. Part 2: Classification and applications. *Computer Methods in Applied Mechanics and Engineering*, 193(39-41):4223–4245, 2004.

[19] J. Mosler and M. Ortiz. On the numerical implementation of variational arbitrary lagrangian-eulerian (vale) formulations. *International Journal for Numerical Methods in Engineering*, 2006. (in press).

[20] M.-C. Rivara. Local modification of meshes for adaptive and / or multigrid finite-element methods. *Journal of Computational and Applied Mathematics*, 36:79–89, 1991.

[21] M.-C. Rivara and Ch. Levin. A 3-D refinement algorithm suitable for adaptive and multigrid techniques. *Communications in Applied Numerical Methods*, 8:281–290, 1992.

[22] E. Bänsch. Local mesh refinement in 2 and 3 dimensions. *Impact of Computing in Science and Engineering*, 3:181–191, 1991.

[23] M.-C. Rivara. New longest-edge algorithms for the refinement and/or improvement of unstructured triangulations. *International Journal for Numerical Methods in Engineering*, 40:3313–3324, 1997.

[24] C. Miehe. Strain-driven homogenization of inelastic microstructures and composites based on an incremental variational formulation. *International Journal for Numerical Methods in Engineering*, 55:1285–1322, 2002.

[25] C. Carstensen, K. Hackl, and A. Mielke. Non-convex potentials and microstructures in finite-strain plasticity. *Proc. R. Soc. Lond. A*, 458:299–317, 2002.

[26] J. Mosler. *On the numerical modeling of localized material failure at finite strains by means of variational mesh adaption and cohesive elements*. Habilitation, Lehrstuhl für Technische Mechanik, Ruhr University Bochum, Germany, 2006.

[27] Y. Kallinderis and P. Vijayant. Adaptive refinement-coarsening scheme for three-dimensional unstructured meshes. *American Institute of Aeronautics and Astronautics Journal*, 31(8):1440–1447, 1993.

[28] J.F. Molinari and M. Ortiz. Three-dimensional adaptive meshing by subdivision and edge-collapse in finite-deformation dynamic plasticity problems with application to adiabatic shear banding. *International Journal for Numerical Methods in Engineering*, 53:1101–1126, 2002.

[29] A. M. Cuitiño and M. Ortiz. A Material-Independent Method for Extending Stress Update Algorithms from Small-Strain Plasticity to Finite Plasticity with Multiplicative Kinematics. *Engineering Computations*, 9:437–451, 1992.

[30] O.T. Bruhns, H. Xiao, and A. Meyers. Constitutive inequalities for an isotropic elastic strain energy function based on hencky's logarithmic strain tensor. *Proc. Roy. Soc. London, A*, 457:2207–2226, 2001.

[31] M. Ortiz and J.J. Quigley. Adaptive mesh refinement in strain localization problems. *Computer Methods in Applied Mechanics and Engineering*, 90:781–804, 1991.